Wave-attenuation characteristics of combined-vegetation wave break forests for big rivers with large flood water level changes

Jie Ren, Zengchuan Dong, Dawei Jin, Yue Zhou, Wei Xu and Biao Sun

ABSTRACT

For large rivers with a compound cross section, the downstream channel has a very wide water surface during the flood season. A wide water surface, high water level, and larger wind speed will cause higher waves, increasing the threat of flooding to the dike. The design of a combined-vegetation wave break forest was put forward to achieve better wave attenuation effect. The main idea of this concept is to plant different types of vegetation at different locations in front of the dike. Three single-vegetation and four combined-vegetation forest schemes were tested under seven different water depth conditions. Both physical experiments and wave numerical simulations were carried out for each scheme to study the wave attenuation effect. The results showed that the wave attenuation effect of the single-vegetation wave break forest was significantly different under different water depth conditions, and the overall effect of the combined-vegetation of wave forest was better. Combined-vegetation wave break forests combine the advantages of different types of vegetation in different water levels, which makes it more economical and reasonable to plant by rivers with large water level variation. The proposed design ideas and methods could provide theoretical support for ecological revetment engineering of large rivers and insights for practical applications.

Key words | combined-vegetation wave break forest, numerical simulation, physical experiment, water level change, wave attenuation

Jie Ren
Zengchuan Dong (corresponding author)
Dawei Jin
Yue Zhou
Wei Xu
Biao Sun
College of Hydrology and Water Resources,
Hohai University,
No. 1, Xikang Road,
Nanjing 10098,
China
E-mail: *zcdong@hhu.edu.cn*

Dawei Jin
Water Resources Department of Jiangsu Province,
No. 5, Shanghai Road,
Nanjing 210029,
China

Wei Xu
River and Lake Protection Center,
Ministry of Water Resources,
No. 3, Yuyuantan South Road,
Beijing 100038,
China

Biao Sun
Water Resources Department of Heilongjiang Province,
No. 4, Wenzhong Road,
Harbin 150001,
China

HIGHLIGHTS

- A new type of wave break forest – combined-vegetation wave break forest – was proposed.
- Plants of different sizes and stiffnesses and different water depth were selected to test different design schemes.
- Each scheme was tested using physical experiments and numerical simulations, and the mean value of the two was taken as the result.

INTRODUCTION

Ecological dike protection is an effective method to reduce the utilization or the size of hard structure revetments. A wave break forest is a type of ecological revetment, which can (1) reduce wave height, (2) improve the ecological environment and regional microclimate, and (3) enhance the stability of the local ecosystem in a coastal zone. Various aspects of wave break forests have been studied, including the hydrodynamics of vegetated areas (Nepf 2012; Kalra *et al.* 2017), the relationship among flow alteration, riparian vegetation and ecosystem (Shafroth *et al.* 2017; Datta 2018), and wave attenuation by vegetation (Kobayashi *et al.* 1993;

doi: 10.2166/wst.2021.011

Nepf 2012; Silinski *et al.* 2018). Wave break forests used to be common on the coast (Sanchez-Nunez *et al.* 2019; Willemsen *et al.* 2020). In recent years, they have also been part of levee revetment construction by rivers and lakes to reduce wave energy and thus reduce damage to levees (Wang 2018; Wenjia Li 2019). However, most of the research on planting wave break forests along rivers and lakes is still in the empirical research stage.

The research on the wave-attenuation effect of wave break forests can be categorized as prototype observation, physical experiment or numerical simulation. Prototype observation is mainly restricted by the environment, so most of the studies are based on physical experiments and numerical simulations. De Reinout (2010) used the SWAN-VEG model to reveal that more, wider, higher or stiffer vegetation results in lower wave heights behind it. Peruzzo *et al.* (2018) used experimental methods to study the effects of immersion ratio and stem density on drag coefficient.

It is widely accepted that wave attenuation by vegetation is related to plant characteristics (width, density, and stiffness) and hydrodynamic conditions (water depth, wave period, and wave height). The wave height at the front of the forest (facing the incoming wave direction) rapidly attenuates wave energy, and then the attenuation rate slows (Knutson *et al.* 1982). Compared with submerged plants, above-ground plants have a greater impact on the water body (Augustin *et al.* 2009). The vegetation density positively impacts the wave energy dissipation (Moeller *et al.* 2014; Silinski *et al.* 2018). For rigid wave break forests, different arrangement modes have different wave attenuation effects (Ren *et al.* 2019). It can be concluded that tree height, forest belt width, arrangement mode and density are the main factors that affect the wave attenuation effect of wave break forests under certain incoming wave conditions. The crown of a rigid wave break forest also plays a major role in the wave attenuation effect. However, most studies have focused on a single plant community and analyzed the effect of its vegetation characteristics on wave attenuation. When studies have involved multiple types of plants, each type is still studied separately.

For some large rivers, the water flows in the main channel and the beach at the same time during a flood, increasing the width of the water surface to more than 10 km. The wide water surface combined with deep water will form larger waves under the action of wind, posing a greater threat to the embankment. Therefore, some large river management departments have also begun to plant dozens of metres of vegetation on the beach near the front of the embankment to prevent waves (Zhang 2015; Jie Ren *et al.* 2019).

A single type of vegetation can only attenuate waves within a certain range of water levels, barely achieving the aim of the construction of the wave break forest, which is to reduce the impact of waves on dikes when there are floods especially for rivers with large variations in water level. For example, if the vegetation height is selected according to the flood situation of a 50-year return period, the water level will only reach the tree trunks in most years. The contribution of tree trunks to wave attenuation is small, which makes it impossible for a wave prevention forest with a single type of vegetation to maximize the wave attenuation effect in most cases. If the tree height is selected according to the flood conditions of a 5-year return period, the crown will be completely submerged by the water level that occurs once in 50 years, thereby failing to protect the dike. Based on the omissions in current research, we reasonably conjectured that compared with the single-vegetation wave break forest, the combined-vegetation wave break forest, with smaller plants placed in front of larger trees with well-developed roots could play a more sustainable role in attenuating waves of different heights.

In order to fully utilize the function of wave break forests under dynamic water levels, the concept of combined-vegetation wave break forest was proposed in this study: different types of plants arranged on the beach of a river along its cross section. This is an improvement on previous single-vegetation wave break forests. Physical model experiments and numerical simulations were carried out on different schemes to study the wave attenuation characteristics of the combined-vegetation wave break forest. In this work, we (1) introduced the scheme design, (2) conducted the physical experiment and numerical simulation, and (3) compared and analyzed the wave attenuation effect of different schemes under different water depth conditions.

METHODS

Scheme design

Physical experiments followed by numerical simulations were carried out and the results of the two were compared to verify each other. Then the mean value of the experimental and computational results was taken as the final result. The physical experiments and the numerical simulations were based on historical data and field investigation of the Baidajie Dike on the lower sub-basins of the Nenjiang River (Wu *et al.* 2020), which is the largest tributary of the Songhua River and its northern source. The Nenjiang is

located in northeastern China and is the boundary river of Inner Mongolia, Heilongjiang and Jilin provinces. The climate of the Nenjiang River Basin is strongly seasonal (Li *et al.* 2014). Precipitation is mainly concentrated in June-September, accounting for 82% of the annual precipitation (Wenjia Li 2019). The average slope of the reach of Baidajie is 0.6 ‰, and the water surface can be 20 km wide in the flood season. According to the 'Preliminary Design Report of the Mainstream Treatment Project of Nenjiang River in Heilongjiang Province' (Heilongjiang Provincial Water Conservancy and Hydroelectric Power Investigation 2015), the flood prevention standard of Baidajie Dike was a 30-year reoccurrence before 2016, which is expected to be raised to a 50-year reoccurrence in the next few years. A sketch of Baidajie Dike is shown in Figure 1, and its hydrologic characteristics and wave features are shown in Table 1. The water depth of the floodplain in Table 1 is the average water depth of floodplain when the designed flood frequency $P = 2\%$. The average wave height and the average wave period were calculated by the Putian experimental station formula, which is recommended by Specification JTS145-2-2013 of China. By this specification, the significant wave height was then calculated according to the average wave height and the average wave period. Currently, poplars and willows are planted on the floodplain along Baidajie Dike, and the total length of vegetation along the river floodplain on the Baidajie's embankment is 2 km. The planned new wave break forest is 10 km.

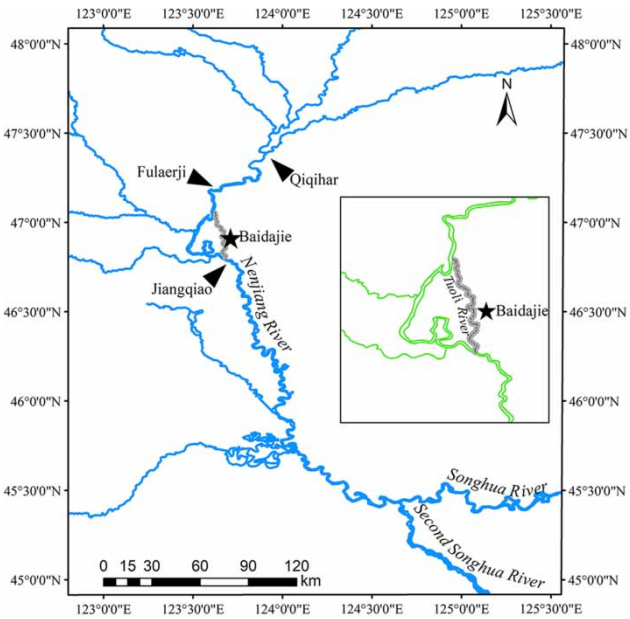

Figure 1 | Sketch of Baidajie Dike.

Table 1 | Wind and wave characteristics of 50-year reoccurrences at Baidajie

Water depth d (m)	Wind speed V (m/s)	Wind direction	Significant wave height H_s (m)	Wave period T (s)
2.83	13	SW	0.91	3.01

Three kinds of single-vegetation wave break forest wave attenuation tests and four kinds of combined-vegetation wave break forest wave attenuation tests were conducted. The three single-vegetation trees were small tree, big tree and flexible vegetation (to simulate flexible plants such as reeds); the small tree was set as 2.4 m tall, big tree 5.2 m and the flexible vegetation was 3 m tall. The four combined-vegetation schemes were divided into two types: rigid (small trees in front of big trees) and flexible–rigid (flexible vegetation in front of rigid vegetation). The specific test scheme parameters are shown in Table 2, and the arrangement is shown in Figure 2.

The rate of increase of the wave attenuation effect begins to decrease at a width of 40 m (Jianting Wang 2018). A wave break forest that is too wide has a certain negative impact on the flood discharging of the river (Jie Ren *et al.* 2019). Therefore, the width of the wave break forest used was 40 m. Seven different water levels (Table 3) were set to simulate the wave attenuation effect of all the schemes. For each scheme under each water depth condition, two physical experiments and two numerical simulations were carried out. The mean of the four was taken as the result. If there were outliers, the outliers were removed before the rest were averaged.

The wave attenuation coefficient was used to measure the wave attenuation effect of the wave break forest of all schemes. The formula of the wave attenuation coefficient is shown in Equation (1) The larger the wave attenuation coefficient, the better the wave attenuation effect of the scheme.

$$K = \frac{H_0 - H_v}{H_0} \times 100\% \tag{1}$$

where K is the wave attenuation coefficient, H_0 is the wave height at a certain site without vegetation and H_v is the wave height at the same site as H_0 with vegetation in front of it.

Physical model

The experiment was conducted in a 70-m-long irregular wave flume in the Hohai University Coastal Engineering Experiment Hall. The flume is 1.0 m wide and 1.8 m

Table 2 | Model parameters

Scheme	Vegetation type	Vegetation height/m	Forest width/m	Arrangement	Vegetation density/(number/m^2)
1	Small rigid tree	2.4	40	Equilateral triangle	0.17
2	Big rigid tree	5.2	40	Equilateral triangle	0.17
3	Flexible vegetation	3	40	Square	49
4	Small + big	2.4 + 5.2	10 + 30	Equilateral triangle	0.17
5	Small + big	2.4 + 5.2	20 + 20	Equilateral triangle	0.17
6	Flexible + big	3 + 5.2	10 + 30	Square + equilateral triangle	49 + 0.17
7	Flexible + big	3 + 5.2	20 + 20	Square + equilateral triangle	49 + 0.17

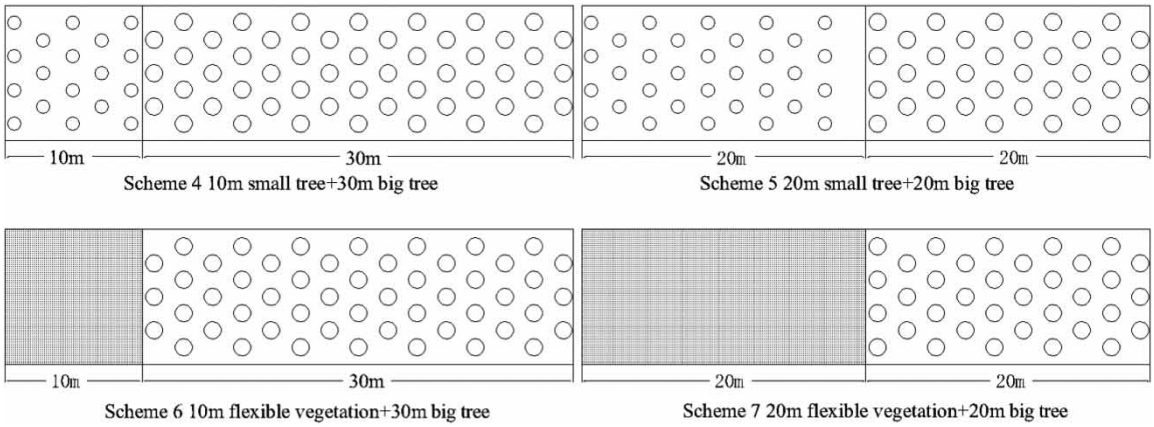

Figure 2 | Sketch of the four combined-vegetation schemes.

Table 3 | Experimental water depth conditions

Class	Water depth/m	Explication of water depth
1	1.52	The water depth when the flood condition is $P = 20\%$
2	2.21	$P = 10\%$
3	2.55	$P = 5\%$
4	2.83	$P = 2\%$
5	2.99	$P = 1\%$
6	3.11	1.1 × the water depth when the flood condition $P = 2\%$
7	3.29	1.1 × the water depth when the flood condition $P = 1\%$

high. One end of the water tank was installed with an irregular wave generator which can simulate regular and irregular waves with a maximum wave height of 0.3 m and wave period of 0.5–5 seconds. A gray concrete plate was laid on the bottom of the water tank, and holes were punched in the gray plastic plate to fix the model plants. At the other end of the tank was a wave dissipation layer, to absorb the wave energy of the coda wave effectively and avoid the interference of the wave reflection to the experiment. A total of five wave height sensors were installed, the first one in front of the wave break forest, with the other four at 1 m intervals into the forest. The experiment layout and the actual scene map are shown in Figure 3.

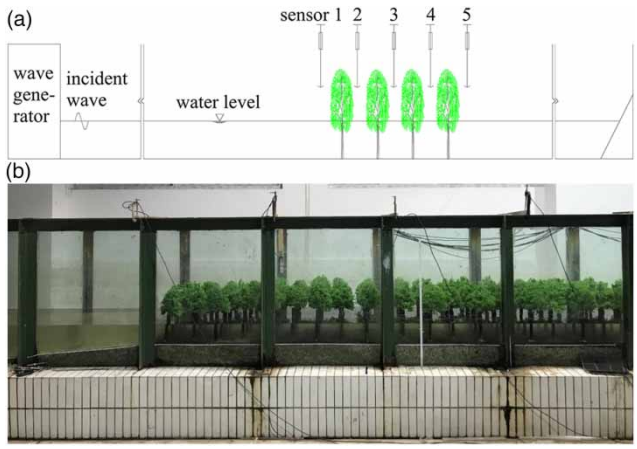

Figure 3 | Sketch of experimental channel layout (a) and side view of experimental scenery (b).

The sensors were connected to a DJ800 acquisition system, feeding the wave surface line data to the computer. The system automatically iterated and modified if the error rate of wave heights between the measured value at the first sensor and the set value exceeded 5%, otherwise the parameters were stored to generate waves. The length scale was set as 10:1 taking account of the actual conditions of vegetation, the wave elements and the existing experimental equipment conditions. Other scales, such as time scale, were set according to gravity similarity criteria.

Three types of model vegetation were prepared, namely flexible vegetation, small rigid tree and large rigid tree. The flexible model vegetation was made of flexible PVC filaments with a height of 30 cm; the rigid model trees were made of a wooden stick for the trunk and plastic for the crown. The trunk of the big tree was 24 cm high and the crown was 28 cm high. The trunk of the small tree was 8 cm high and the crown was 16 cm high. The models are shown in Figure 4.

All the physical experiments in this study were carried out using irregular waves, in accordance with Specification JTS145-2-2013 of China. Experiments were validated by the significant wave height, which is described by the following expression:

$$H_{1/3} = \frac{1}{N/3}\sum_{j=1}^{N/3} H_j \tag{2}$$

where H_j is the value of the wave height counted by the zero-up crossing method.

Mathematical model

The main idea of the mathematical model was to generate an unstructured triangular computing grid using the Surface Water Modeling System (SMS), and to simulate the wave attenuation effect of the wave break forest by building a SWAN wave simulation model based on the unstructured computing grid.

The SMS model was developed by the United States Army Corps of Engineers Hydraulics Laboratory and Brigham Young University to simulate complex river topography and shorelines. It is based on the two-dimensional shallow water equation to simulate and analyze the laws of surface water movement. ADCIRC is one of the finite element modules in SMS. It uses unstructured triangular grids for grid difference and simulation calculations. Compared with structured grids, unstructured grids can better fit complex boundaries, and local encryption grids can be used to meet the calculation accuracy of sensitive areas (Team 2009). Unstructured grids have the advantages of easy network construction and high calculation accuracy and are especially suitable for areas with complex terrain and water depth changes. The grid file generated by SMS can be directly used as an input to the SWAN model, avoiding errors caused by different grids and further improving calculation accuracy.

The SWAN model is based on linear random surface gravity wave theory and full implicit difference. It describes the random wave field with two-dimensional interaction spectral density, and takes the dynamic spectral balance equation as the governing equation. The overall idea is to carry out finite element calculation of the governing

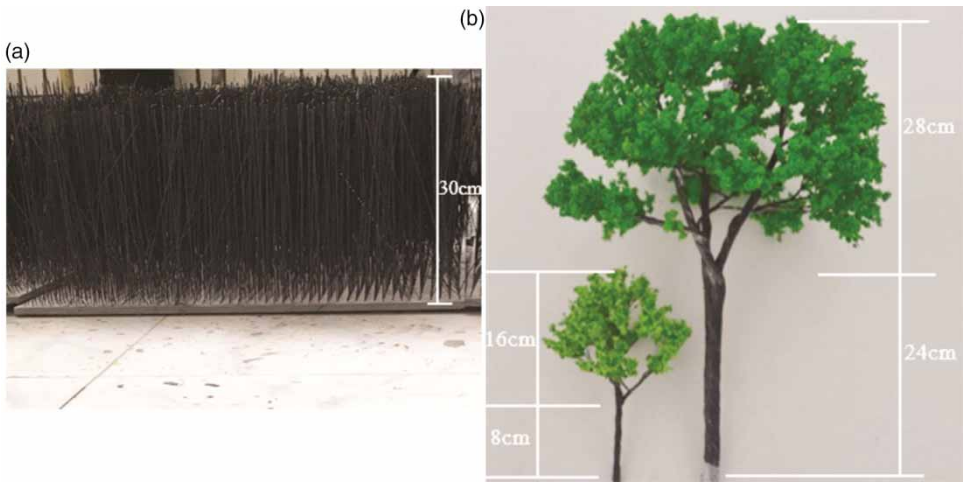

Figure 4 | Flexible model vegetation (a) and rigid model trees (b).

equation in time, space and spectral space after considering refraction, diffraction, dissipation and bottom friction, water depth, wind field and other conditions. This model can simulate wave generation, propagation and dissipation processes. In the SWAN model, vegetation dissipation is achieved by wave energy attenuation through the dissipation rate of wave energy per unit area. In the Cartesian coordinate system, the governing equation of the SWAN model can be expressed as:

$$\frac{\partial}{\partial t}N+\frac{\partial}{\partial t}C_xN+\frac{\partial}{\partial t}C_yN+\frac{\partial}{\partial \theta}C_\theta N+\frac{\partial}{\partial \sigma}C_\sigma N=\frac{S_{\text{tot}}}{\sigma} \quad (3)$$

where N is the dynamic spectral density, the ratio of the spectral density to the relative frequency; C_x is the velocity of a wave in the geographic coordinate space x; C_y is the velocity of a wave in the geographic coordinate space y; C_θ is the velocity of a wave in the relative frequency space θ; C_σ is the velocity of a wave in the relative frequency space σ; $(\partial/\partial t)N$ is change in acting density over time, $(\partial/\partial t)C_xN$, $(\partial/\partial t)C_yN$ is the propagation of wave energy in two dimensions, $(\partial/\partial\theta)C_\theta N$ is the refraction caused by changes in flow field and water depth, $(\partial/\partial\sigma)C_\sigma N$ is changes in angular frequency caused by changes in flow field and water depth; S_{tot} is the source function term that controls the physical process, including wind growth, whitecapping, quadruplets, bottom friction, vegetation dissipation and so on.

River generalization and grid division

According to the embankment data, the boundary of the SMS grid and its attributes were determined. The upper and lower boundaries of the study reach were set as open boundaries, and the two sides were set as land boundaries. Waves at the open boundary can freely enter and exit, and waves at the land boundary are absorbed without generating waves. The overall grid side length was set as 50 m for the two-dimensional triangular grid difference considering the calculation pressure of model and the forest width. The wave break forest and the buffer zone around it was set at 1,500 m long and 200 m wide. The side length of this area was refined to 10 m, and the final unstructured triangular computing grid was obtained. On the basis of the unstructured grid, the water level and terrain data files were imported, and the SMS ADCIRC model was used to generate the bathymetric terrain files. The water depth grid of the once-in-50-year flood in the research area and the partial enlarged image of vegetation area is shown in Figure 5. There are more than 400,000 cells in the grid.

Vegetation file

Vegetation parameters mainly include height, stem width, density and resistance coefficient. Vegetation height and stem width were obtained from the field survey of vegetation in the study area. The vegetation density was determined by the vegetation parameter file and the vegetation grid file (Team 2009). The vegetation model was divided into a trunk layer and a crown layer by layering treatment (Reinout 2010), and the attenuation effects of the two layers were superimposed vertically to obtain the overall attenuation effect. The stiffness of the vegetation was reflected in the resistance coefficients, and the rigid vegetation was layered with different coefficients after layering the crown and trunk, respectively. The values of the stiffness coefficients were preliminarily estimated according to Cao's (2012) formula, and the values were adjusted according to the physical experiment results.

RESULTS AND DISCUSSION

The mutual verification was to compare the wave heights obtained by physical experiments and numerical simulations at the five sensor locations shown in Figure 3. The wave heights obtained by the physical experiments and numerical simulations at each measurement point are shown in Figure 6(a), and the correlation between them is shown in Figure 6(b). The difference between the two groups of results in the corresponding positions is not more than 20%, which could be considered to validate the two kinds of experiments.

Then the seven schemes shown in Table 2 were simulated under seven water depths (Table 3), and the results are shown in Table 4 and Figure 7.

Comparison of different single-vegetation forests

There are significant differences between the wave attenuation effects of the single-vegetation forest with different tree types under the same conditions, as shown in Figure 7(a). The wave attenuation effect of rigid small trees increases first and then decreases with the increase of water depth. The reason for the gradual increase is that before the water depth overtops the small trees, the effective height of the crown for wave attenuation gradually increases, and the wave attenuation effect also increases. After the small trees are submerged, the wave attenuation is significantly reduced. The speed of water particles in a

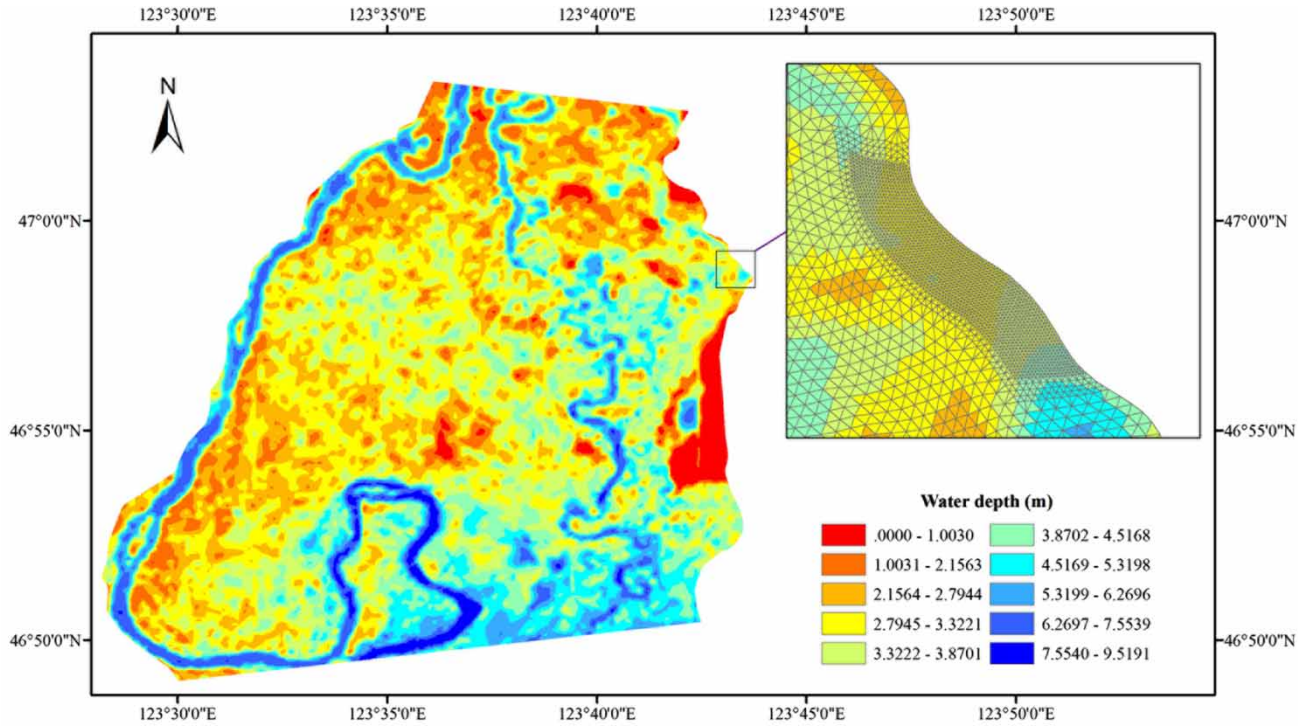

Figure 5 | The water depth grid of the once-in-50-year flood in the research area and the partial enlarged image of the vegetation area.

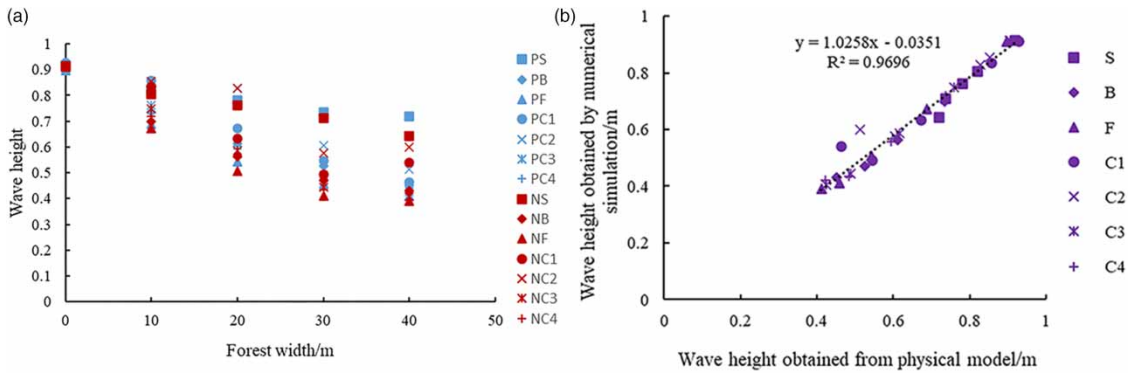

Figure 6 | Wave height of each measuring position for the water level of a 50-year return period (a) and the comparison of results between physical experiments and numerical simulations (b). In the legend, P = physical experiment, N = numerical simulation, S = small tree scheme, B = big tree, F = flexible vegetation and C = combined-vegetation forests.

wave decreases gradually from the water surface downward. Under the same vegetation conditions, the resistance of vegetation to waves decreases gradually from the water surface downward, and the contribution of vegetation to wave attenuation also decreases gradually from the water surface downward. Thus, after the small trees are completely submerged, the vegetation cannot attenuate the upper wave energy, so its contribution to wave energy attenuation was low. However, when the water is level with the crowns of the small trees and the trunks of the big trees, the wave attenuation coefficient of the small trees is greater than that of the big trees, indicating that the wave attenuation effect of the crown of the small trees is better than that of the trunks of the big trees under non-submerged conditions. This is because the dense branches and leaves of the crown approximate to a spherical shape that is porous. The wave propagation on the beach is similar to that of a non-deformed sine wave. When the wave enters the forest, because of the isotropy of the spherical object, the tree crowns have an impact on the waves in all directions, forming effective resistance. In addition, the tree crowns cause many turbulences on a small scale, thus increasing the

Table 4 | Wave attenuation coefficients of different schemes

	Wave attenuation coefficient/%						
Water depth/m	**Scheme 1**	**Scheme 2**	**Scheme 3**	**Scheme 4**	**Scheme 5**	**Scheme 6**	**Scheme 7**
1.52	35.82	30.43	40.73	31.87	33.21	33.04	35.64
2.21	38.01	39.69	48.69	39.36	38.30	42.00	44.20
2.54	27.79	48.64	52.24	43.49	38.68	51.34	50.51
2.83	25.63	52.05	55.52	45.45	38.89	54.26	53.56
2.99	24.53	54.98	55.94	47.42	39.83	55.71	55.53
3.11	22.87	57.50	52.40	48.84	40.11	56.23	55.04
3.29	22.53	58.53	44.74	49.34	40.25	55.15	52.65

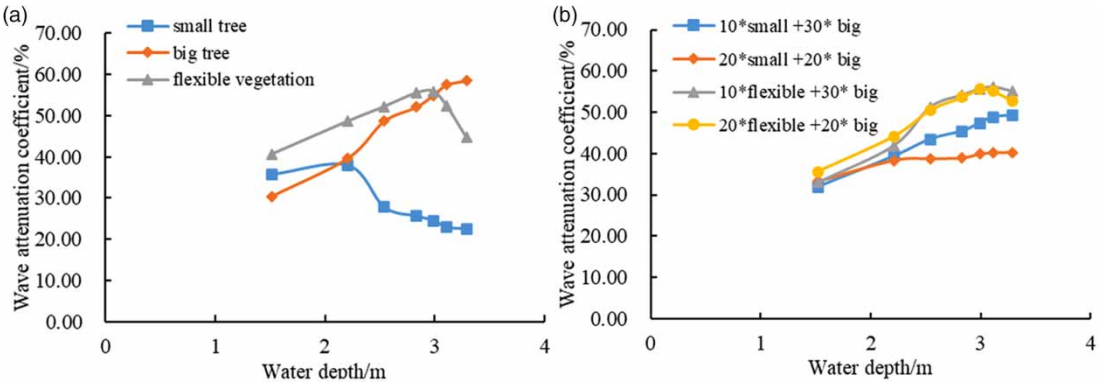

Figure 7 | Wave attenuation coefficients of different single-vegetation forests (a) and combined-vegetation forests (b).

wave energy dissipation. Therefore, at the same water level, the contribution of tree crowns to wave attenuation is clearly greater than that of tree trunks.

The wave attenuation effects of the big trees are enhanced with the increase of water level. On the one hand, the wave attenuation effects are vertical and superimposed. On the other hand, the contribution of tree crown to wave attenuation is greater than that of tree trunk. With the rise of water level, the proportion of the tree crown in wave attenuation increases, meaning that the effect of wave attenuation is non-linear as the water level rises, before submergence.

At low water levels, flexible vegetation can provide all the advantages of high planting density and a large amount of effective vegetation that attenuates waves. The effect of attenuation wave energy of vegetation is superimposed, and the effect of wave attenuation by flexible vegetation is significant. In addition, before the water depth inundates the flexible vegetation, with the increase of water depth, the effective height of wave attenuation gradually increases, and the wave attenuation effect of vegetation also increases. Due to the poor flood tolerance and lodging resistance of the flexible vegetation, when the water depth overtops it, the wave attenuation effect is weakened. Therefore, the wave attenuation coefficient curve of flexible vegetation on its own shows a pattern of first rising and then dropping.

Comparison of different combined-vegetation forests

In scheme 4 ($10 \times$ small $+ 30 \times$ big) and scheme 5 ($20 \times$ small $+ 20 \times$ big), the crown of the small trees and the trunks of the large trees played the major role in wave attenuation for once-in-5-year and once-in-10-year water levels. When the water level is above the height of the small trees and level with the crown of the big trees, wave attenuation is mainly by the crown of the big trees. With the increase of water depth, the effective wave attenuation height of the crown of the big trees gradually increases, and the wave attenuation effect is enhanced with the increase of water depth.

In scheme 6 ($10 \times$ flexible $+ 30 \times$ big) and scheme 7 ($20 \times$ flexible $+ 20 \times$ big), the wave attenuation coefficient of the wave break forest first rises and then falls. When the water level is of a 5-year return period and a 10-year

return period, the densely planted flexible vegetation provides the main contribution to wave attenuation. When the water level is a 20-year return period, a 50-year return period and a 100-year return period, the densely planted flexible vegetation and the crown of the big trees plays the major role in wave attenuation. With the increase of water depth, the effective wave attenuation height of the flexible vegetation and the trees gradually increases, and the wave attenuation effect is also enhanced. However, once the flexible vegetation is submerged, the effect of wave attenuation began to decrease.

In the Baidajie river reach, the wave attenuation effect of the rigid combined-vegetation wave forest is lower than that of rigid and flexible combined-vegetation wave forest. Among the seven layout schemes, scheme 7 ($20 \times$ flexible + $20 \times$ big) is the most suitable for the embankment section of Baidajie. It had a good effect of attenuating waves at both low and high water levels, and thus could play an effective role in protecting the bank.

Combined-vegetation wave break forest design pattern

Based on the above experiments and the analysis of the experimental results, we suggest the following for designing combined-vegetation wave break forests: (1) the vegetation must be able to stay upright under a certain water depth; (2) the wave attenuation part of vegetation needs to have a higher density; (3) the projections of the wave attenuation parts of different plants must have a certain mutual coverage vertically (see Figure 8). The crown of large vegetation h3 should be higher than the height of the design water level superimposed by waves h. The height of flexible vegetation h1 should be greater than the height of the lower edge of the crown of rigid vegetation h2.

CONCLUSIONS

A design for combined-vegetation wave break forests was proposed to fill the gaps in existing research on wave break forests that cannot cope well with water level changes. Physical experiments and numerical simulations were carried out on three single-vegetation and four combined-vegetation schemes. The wave attenuation coefficient of each design scheme was calculated from the mean value of the physical experiment and the numerical simulation. The wave attenuation coefficient curve of each scheme under different water depths and different schemes under the same water depth was compared. A basic understanding of wave attenuation characteristics of combined-vegetation forest was obtained.

The contribution of the crown of rigid vegetation in wave attenuation is clearly greater than that of the trunk layer. This is because the dense branches and leaves make the whole crown approximately spherical and porous. It generates effective resistance to waves and many small-scale turbulences, increasing wave energy dissipation. Due to its thin stems and large planting density, the wave attenuation effect of flexible vegetation is obvious after being combined. But flexible vegetation is not effective at wave attenuation once it is submerged, because of the poor submergence resistance and lodging resistance of flexible vegetation. Therefore, small trees and flexible vegetation contribute little to wave energy attenuation at high water levels.

The wave attenuation effect of the single-vegetation wave break forest is different under different water conditions, and the overall effect of the combined-vegetation wave break forest is better. At low water levels, the combined-vegetation wave break forest provide the benefits of wave attenuation by the crowns of small trees or dense flexible vegetation. At high water levels, the crowns of the large trees can eliminate waves. The combined forest can make comprehensive use of the advantages of various types of vegetation for wave attenuation at different water levels. It improves the wave attenuation effect of rivers with great seasonal variation of water level under most incoming water conditions. A design pattern for combined-vegetation wave break forest was put forward to provide a reference for future wave break forest planning and design.

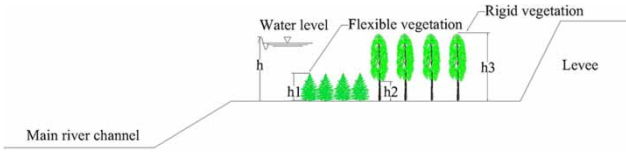

Figure 8 | Design of combined-vegetation wave break forest.

FUNDING

This research was funded by the Applied Technology Research and Development Program of Heilongjiang Province under Grant No. GZ16B031.

DATA AVAILABILITY STATEMENT

All relevant data are included in the paper or its Supplementary Information.

REFERENCES

Augustin, L. N., Irish, J. L. & Lynett, P. 2009 Laboratory and numerical studies of wave damping by emergent and near-emergent wetland vegetation. *Coastal Engineering* **56** (3), 332–340. doi:10.1016/j.coastaleng.2008.09.004.

Cao, H. 2012 *Research on Numerical Modeling of Wave Dissipation by Vegetation with SWAN-VEG*. HoHai University, Nanjing, China.

Datta, D. 2018 Assessment of mangrove management alternatives in village-fringe forests of Indian Sunderbans: resilient initiatives or short-term nature exploitations? *Wetlands Ecology and Management* **26** (3), 399–413. doi:10.1007/s11273-017-9582-7.

Heilongjiang Provincial Water Conservancy and Hydroelectric Power Investigation, D.a.R.I. 2015 *Management Project Preliminary Design Report of the Mainstream of Nenjiang River in Heilongjiang Province, Heilongjiang Provincial Water Conservancy and Hydroelectric Power Investigation*. Design and Research Institute, Harbin.

Jianting Wang, Z. D., Xu, W. & Ren, J. 2018 Influencing factors analysis of wave dissipation of the wavebreak forest in mainstream of Nenjiang River. *Journal of Hohai University (Natural Sciences)* **46** (1), 30–36. doi:10.3876/j.issn.1000-1980.2018.01.005.

Jie Ren, Z. D., Xu, W., Zhou, Y., Wei, Y. & Wang, J. 2019 Study on influence of river wavebreak forest on flood discharge ability based on mike21 fm model. *Journal of Hohai University (Natural Sciences)* **47** (5), 420–424. doi:10.3876/j.issn.1000-1980.2019.05.004.

Kalra, T. S., Aretxabaleta, A., Seshadri, P., Ganju, N. K. & Beudin, A. 2017 Sensitivity analysis of a coupled hydrodynamic-vegetation model using the effectively subsampled quadratures method. *Geoscientific Model Development Discussions* 1–28. doi:10.5194/gmd-10-4511-2017.

Knutson, P. L., Brochu, R. A., Seelig, W. N. & Inskeep, M. 1982 Wave damping in *Spartina alterniflora* marshes. *Wetlands* **2** (1), 87–104. doi:10.1007/BF03160548.

Kobayashi, N., Raichle, A. W. & Asano, T. 1993 Wave attenuation by vegetation. *Journal of Waterway Port Coastal & Ocean Engineering* **119** (1), 30–48.

Li, F., Zhang, G. & Xu, Y. J. 2014 Spatiotemporal variability of climate and streamflow in the Songhua River Basin, Northeast China. *Journal of Hydrology* **514**, 53–64. doi:10.1016/j.jhydrol.2014.04.010.

Moeller, I., Kudella, M., Rupprecht, F., Spencer, T., Paul, M., van Wesenbeeck, B. K., Wolters, G., Jensen, K., Bouma, T. J., Miranda-Lange, M. & Schimmels, S. 2014 Wave attenuation over coastal salt marshes under storm surge conditions. *Nature Geoscience* **7** (10), 727–731. doi:10.1038/ngeo2251.

Nepf, H. M. 2012 Hydrodynamics of vegetated channels. *Journal of Hydraulic Research* **50** (3), 262–279. doi:10.1080/00221686.2012.696559.

Peruzzo, P., De Serio, F., Defina, A. & Mossa, M. 2018 Wave height attenuation and flow resistance due to emergent or near-emergent vegetation. *Water* **10** (4). doi:10.3390/w10040402.

Reinout, O. d. 2010 *Modelling Wave Attenuation by Vegetation with Swan-veg; Model Evaluation and Application to the Noordwaard Polder*. University of Twente, Delft.

Ren, J., Dong, Z., Xu, W., Zhang, Q., Shi, R., Zhu, H. & Sun, B. 2019 Multi-objective optimization of wave break forest design through machine learning. *Journal of Hydroinformatics* **21** (2), 295–307. doi:10.2166/hydro.2019.072.

Sanchez-Nunez, A. D., Bernal, G. & Mancera Pineda, J. E. 2019 The relative role of mangroves on wave erosion mitigation and sediment properties. *Estuaries and Coasts* **42** (8), 2124–2138. doi:10.1007/s12237-019-00628-9.

Shafroth, P. B., Schlatter, K. J., Gomez-Sapiens, M., Lundgren, E., Grabau, M. R., Ramirez-Hernandez, J., Rodriguez-Burgueno, E. J. & Flessa, K. W. 2017 A large-scale environmental flow experiment for riparian restoration in the Colorado River Delta. *Ecological Engineering* **106**, 645–660. doi:10.1016/j.ecoleng.2017.02.016.

Silinski, A., Schoutens, K., Puijalon, S., Schoelynck, J., Luyckx, D., Troch, P., Meire, P. & Temmerman, S. 2018 Coping with waves: plasticity in tidal marsh plants as self-adapting coastal ecosystem engineers. *Limnology & Oceanography* **63** (2), 799–815. doi:10.1002/lno.10671.

Team, T. S. 2009 *SWAN User Manual*. Delft University of Technology, The Netherlands.

Wang, S. 2018 *Design of Recover Green Project of the Yangtze River Bank in Junshan District, Hunan*. Central South University of Forestry and Technology, Changsha Hunan.

Wenjia Li, Z. L. 2019 Demonstration and formation of standardized embankment in the lower reaches of the Yellow River. *Yellow River* (10), 53–57. doi:10.3969/j.issn.1000-1379.2019.10.010.

Willemsen, P. W. J. M., Borsje, B. W., Vuik, V., Bouma, T. J. & Hulscher, S. J. M. H. 2020 Field-based decadal wave attenuating capacity of combined tidal flats and salt marshes. *Coastal Engineering* **156**. doi:10.1016/j.coastaleng.2019.103628.

Wu, Y., Zhang, G., Rousseau, A. N., Xu, Y. J. & Foulon, É. 2020 On how wetlands can provide flood resilience in a large river basin: a case study in Nenjiang River Basin, China. *Journal of Hydrology* **587**. doi:10.1016/j.jhydrol.2020.125012.

Zhang, M. 2015 Planting of wavebreak forest in middle reaches of Huaihe River: influential factors and selection of tree species. *China Water Resources* (09), 22–24.

First received 14 September 2020; accepted in revised form 26 December 2020. Available online 6 January 2021